Ultracold atoms in one-dimensional optical lattices approaching the Tonks-Girardeau regime

Pollet, L.; Rombouts, S.M.A.; Denteneer, P.J.H.

Ultracold Atoms in One-Dimensional Optical Lattices Approaching the Tonks-Girardeau Regime

L. Pollet,[1,*] S. M. A. Rombouts,[1] and P. J. H. Denteneer[2]

[1]*Vakgroep Subatomaire en Stralingsfysica, Universiteit Gent, Proeftuinstraat 86, 9000 Gent, Belgium*
[2]*Instituut-Lorentz, Universiteit Leiden, P.O. Box 9506, 2300 RA Leiden, The Netherlands*

Recent experiments on ultracold atomic alkali gases in a one-dimensional optical lattice have demonstrated the transition from a gas of soft-core bosons to a Tonks-Girardeau gas in the hard-core limit, where one-dimensional bosons behave like fermions in many respects. We have studied the underlying many-body physics through numerical simulations which accommodate both the soft-core and hard-core limits in one single framework. We find that the Tonks-Girardeau gas is reached only at the strongest optical lattice potentials. Results for slightly higher densities, where the gas develops a Mott-like phase already at weaker optical lattice potentials, show that these Mott-like short-range correlations do not enhance the convergence to the hard-core limit.

I. Introduction.—Since the prediction by Jaksch *et al.* [1] on the experiment by Greiner *et al.* [2], ultracold atoms in optical lattices have been the focus of much activity. By tightly confining the motion in the transverse direction, an array of quasi-one-dimensional optical lattices results [3], where particle exchange between the one-dimensional tubes is suppressed. The role of quantum fluctuations is enhanced in one dimension compared to the three-dimensional case, such that traditional mean-field theories fail. Instead, the long-range low-energy physics is described by the Luttinger liquid model. In the limit of infinite repulsion between the atoms the atomic gas is called a Tonks-Girardeau gas [4,5] (TG). Because of the blocking of double occupancies, the resulting hard-core bosons have some properties very similar to noninteracting fermions; e.g., the density profiles become indistinguishable. However, more complicated properties such as the momentum distribution remain discriminating characteristics [6]. The regime of strong repulsions between bosons has been studied experimentally [7] and theoretically [8] for an atomic gas not subject to an optical potential, but the acquired values for the ratio of the repulsive interaction strength to the kinetic energy were rather low and the TG regime was not seen. By using an optical lattice, much higher values for this ratio could be reached [6]. The interpretation of these experiments is complicated by the finite-size effects due to the harmonic trap. But even in the homogeneous case, an accurate theoretical description of the transition from a weakly interacting Bose gas to a strongly interacting Tonks gas has to rely on numerical simulations. Our aim is to model the experimental results of Ref. [6] using one single numerical framework which accommodates both the weakly and the strongly interacting regime.

The physics of ultracold atoms in optical lattices can be described by the Bose-Hubbard model [1], which considers bosons occupying Wannier orbitals. The validity of this model is confirmed by the ratio of the central to first

Bragg peak in the experimentally observed momentum distributions, which depends only on the shape of the Wannier orbitals (see below). The TG regime is characterized by the absence of double occupancies in the many-boson wave function. To identify the TG regime unambiguously, one has to evaluate whether the experimental results are better described by soft-core bosons with a considerable overlap or by hard-core bosons for which double occupations are explicitly suppressed. Exact results for realistic parameters over the entire range of the axial optical lattice depths used in the experiment are obtained using quantum Monte Carlo methods. We find that the results for soft-core and hard-core bosons do not coincide except for the strongest optical potentials used in the experiments, in contrast with the fermionization approach of Ref. [6] which assumes hard-core bosons at all optical-potential strengths.

II. One-dimensional optical lattice.—When an ultracold Rb gas of atoms is cooled and loaded into an optical lattice [2] with very tight transverse confinement, its dynamics is governed by the one-dimensional Hamiltonian,

$$H = \frac{p^2}{2m} + V_0(x) + V_T(x) + g_{\text{int}}\sum_{i<j}\delta(x_i - x_j), \quad (1)$$

with m the atomic mass, x_i the position of atom i, $V_0(x) = V_0\sin^2(kx)$ the optical potential (V_0 takes the laser intensity and the dynamic polarizability of the atoms into account), and $V_T(x)$ the harmonic trapping potential, which varies slowly compared to the optical potential. The wave vector k of the laser along the axial direction defines the length scale $\lambda/2$ through $k = 2\pi/\lambda$ and the recoil energy $E_R = \hbar^2 k^2/(2m)$ which we will use as an energy scale. The Hamiltonian Eq. (1) reduces to the exactly solvable Lieb-Liniger [5] model for $V_T(x) = 0$ and $V_0(x) = 0$ while it reduces to a Mathieu equation for $V_T(x) = 0$ and $g_{\text{int}} = 0$. The interaction g_{int} between the

atoms is determined by the three-dimensional scattering length a_s of the atoms. Olshanii [9] studied the scattering problem of two particles in tight waveguides and found for the effective one-dimensional coupling constant

$$g_{int} = \frac{2\hbar^2 a_s}{m a_\perp^2} \frac{1}{1 - 1.033 a_s/a_\perp}, \quad (2)$$

where $a_\perp = \sqrt{\hbar/m\omega_\perp}$ is the characteristic length of the transverse harmonic confinement. For very tight radial confinement it suffices to integrate over the y and z directions assuming harmonic confinement, yielding $g_{int} = \frac{2\hbar^2 a_s}{m a_\perp^2}$. The Wannier orbitals are calculated for the periodic potential given by the kinetic and the optical terms in Eq. (1), restricted to the lowest band [10]. For low-density gases we can express the Hamiltonian of Eq. (1) in the Wannier basis, resulting in a Bose-Hubbard model [1,11],

$$H = -J \sum_{\langle i,j \rangle} b_i^\dagger b_j + \sum_i \varepsilon_i n_i + \frac{U}{2} \sum_i n_i(n_i - 1), \quad (3)$$

where the first summation runs over nearest neighbors only, the operator n_i counts the number of bosons at site i and the effective parameters U, ε_i, and J represent the strengths of the on-site repulsion, the harmonic trapping, and the kinetic hopping, respectively. Recent studies of the one-dimensional Bose-Hubbard model mainly focused on the Mott-superfluid transition, using a wide range of methods: a slave-boson approach [12], the numerical renormalization group [13], the density matrix renormalization group [14], the time-evolving block decimation method [15], and Monte Carlo methods [16]. The main uncertainties in the model relate to the accuracy of the scattering length a_s and the renormalization of the effective parameters of the Bose-Hubbard model. As we work in the grand-canonical ensemble, the chemical potential μ must be fine-tuned such that the expected number of particles corresponds to the experimental number of particles. The Bose-Hubbard model is simulated using the stochastic series expansion method [17] (SSE) with locally optimized directed loop updates [18,19]. From this Monte Carlo simulation thermodynamic observables such as the energy, the (local) density, the (local) compressibility, and the one-body correlation function can be computed exactly in a statistical sense [20].

III. Homogeneous system.—First, we consider a homogeneous ($\varepsilon_i = 0$) atomic gas in a lattice of $L = 128$ sites with periodic boundary conditions at a very low but finite temperature, $T/J = 0.2$. In Fig. 1 we show the internal energy per site of this system for increasing values of U/J, keeping the average density fixed at $\langle n \rangle \approx 0.5$. An ideal Bose gas occurs in the limit of vanishing U, which is indicated by the lower horizontal line in Fig. 1, while the ideal Fermi gas is found for $U \to \infty$ and indicated by the upper horizontal line. For very large values of U/J, no site of the lattice will be doubly occupied and one can
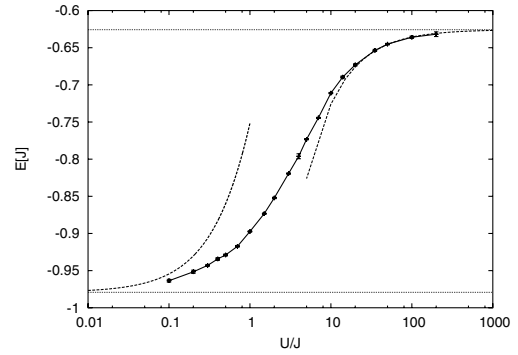

FIG. 1. Internal energy per site as a function of U/J for a homogeneous model with 128 sites at a temperature $T/J = 0.2$. The data points with error bars connected by the full line are the energies obtained by the SSE method. The energies for noninteracting fermions (upper dotted horizontal line) and noninteracting bosons (lower dotted horizontal line) are shown, together with the Bogoliubov approximation for bosons (dashed line on the left) and a first-order perturbation theory for fermions (dashed line on the right).

apply the Jordan-Wigner transformation to map the bosons onto fermions [21]. For small but finite U ($U/J \ll 0.1$ in Fig. 1) , the system is adequately described by the standard Bogoliubov approximation [10]. For large U a perturbation of interacting fermions was derived in Ref. [22] to order $1/U$. From the log scale in Fig. 1 it appears that the limit of noninteracting fermions is reached slowly for values of $U/J > 10$. For $U/J \sim 1$ one has to resort to numerical methods, and we see that the SSE method remains efficient over the entire U/J range. Higher temperatures lead qualitatively to the same results, but the description in terms of fermions is only valid for higher values of U/J. Temperature can be seen as a source for exciting double occupancy on a particular site, whose likeliness must be suppressed by a stronger on-site repulsion term.

IV. Inhomogeneous system.—The harmonic trapping potential breaks the homogeneity of the system. For the parameters we follow Ref. [6]: the scattering length a_s of Rb atoms is taken to be $a_s = 102(6)a_0$ [23], with a_0 the Bohr length; the characteristic length $a_\perp$ of the tight confinement in the y and z directions is $a_\perp = 57.6$ nm; the parameter ε_i in Eq. (3), characterizing the trapping in the axial direction, is given by $\varepsilon_i = \int dx V_T(x)|\Psi(x - x_i)|^2 \simeq 8 \times 10^{-4} E_R(i - \frac{L}{2})^2$, with $\Psi(x - x_i)$ the Wannier function centered around site i and $L = 50$ the total number of sites. The ratio U/J can be varied by changing the optical-potential strength V_0. The temperature T and the number of particles in one tube are not directly accessible experimentally. The averaging over an array of one-dimensional tubes in Ref. [6] can be understood as an averaging over condensates with different temperatures and particle numbers. However, one can understand the onset of the TG limit from simulations for a single tube with a fixed temperature. We used $T/J = 1$ at all

interaction strengths, which is of the same order as the temperatures estimated in Ref. [6]. In Fig. 2 the local densities and the momentum profiles are shown for several values of the optical-potential strength V_0, in line with the actual values used in the experiment of Ref. [6]. All Monte Carlo simulations consist of at least 20 chains of 2^{16} samples with each 50–200 off-diagonal updates such that error bars are not visible.

Momentum profiles are experimentally measurable and can be calculated from a numerical simulation as

$$n(p) = |\Phi(p)|^2 \sum_{j,l} e^{-ip(j-l)} \langle b_j^\dagger b_l \rangle, \qquad (4)$$

where the envelope $\Phi(p)$ is the Fourier transform of the Wannier function $\Psi(x)$, p denotes momentum in units of $\hbar k$, and $\langle b_j^\dagger b_l \rangle$ is the one-body density matrix of the Bose-Hubbard model. In Fig. 2, the peak observed at $p = 2\hbar k$ is the first-order diffraction peak reflecting the presence
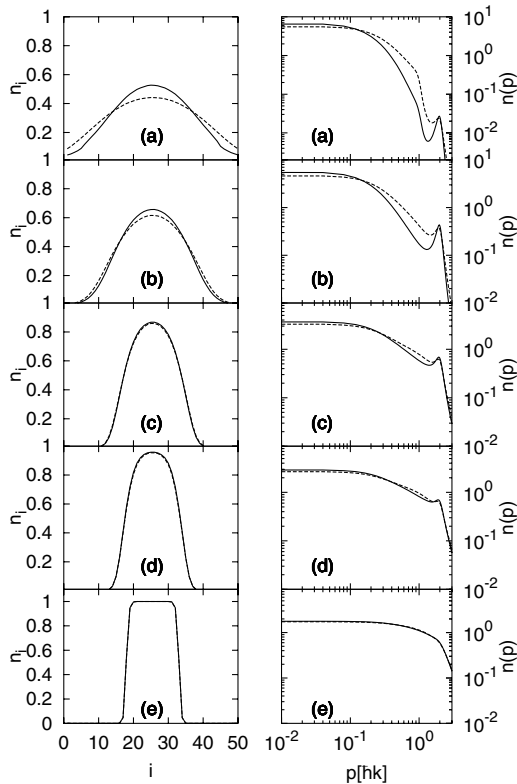

FIG. 2. Local densities n_i in coordinate space as a function of the site index i (left) and the corresponding momentum profiles $n(p)$ as a function of the momentum p (in units $\hbar k$) on the right. The axial optical lattice depths, the ratios U/J and the values of the slope parameter α for soft-core (solid line) and α' for hard-core bosons (dashed line) are (a) $V_0/E_R = 1$, $U/J = 1.75$, $\alpha = 2.71$, $\alpha' = 1.69$, (b) $V_0/E_R = 5$, $U/J = 7.85$, $\alpha = 1.92$, $\alpha' = 1.38$, (c) $V_0/E_R = 9.5$, $U/J = 28.6$, $\alpha = 1.00$, $\alpha' = 0.78$, (d) $V_0/E_R = 12$, $U/J = 52.28$, $\alpha = 0.72$, $\alpha' = 0.56$, (e) $V_0/E_R = 20$, $U/J = 258.54$, $\alpha = 0.33$, $\alpha' = 0.32$. In each plot the average number of particles is $\langle N \rangle \approx 15$, the temperature is $T/J = 1$, and the lattice consists of 50 sites.

of the optical lattice. The ratio between the height of the central peak and the first-order peak is solely related to the width of the Wannier orbitals and is not affected by averaging over the array of tubes or by the dynamics of the Bose-Hubbard model. The procedure to calculate the Wannier orbitals outlined above yields ratios in good agreement with the experimental data shown in Fig. 2 of Ref. [6]. This suggests that the ramping down along the axial direction in the experiment proceeded adiabatically, and it demonstrates that the discrete Bose-Hubbard model is a valid approach to describe the physics of ultracold atomic alkali gases in optical lattices.

In each of Figs. 2(a)–2(e) there is a region where the slope of the momentum distribution is almost linear (on a log-log scale), similar to what occurs in an infinite homogeneous Tonks gas at $T = 0$, which has an infrared divergence $n(p) \propto p^{-1/2}$ at low momenta and an asymptotic tail $n(p) \propto p^{-4}$ at high momenta [24]. In our case, the periodicity of the optical lattice sets an upper momentum scale $p_L = \hbar k$. The width of the Wannier orbitals sets another upper scale, $p_W \simeq (V_0/E_R)^{1/4} p_L$, which turns out to be larger than p_L for the parameter regimes considered here. The harmonic trap sets a lower momentum scale $p_T = (m\hbar\omega)^{1/2} \simeq 0.1\hbar k$, below which the momentum distribution is flattened because of the suppression of long-range correlations. Because of the trapping potential, the influence of temperature on the momentum distribution will be different from the homogeneous case: thermal fluctuations will occur at the edges of the cloud and therefore they will mainly affect the momentum distribution below p_T. Only the momentum distribution in the region between p_T and p_L relates directly to the short-range dynamics of the Bose-Hubbard model and might show a power-law behavior similar to the homogeneous system. We have fitted the linear parts of the log-log curves in this region with a power-law $n(p) \propto p^{-\alpha}$. The slope α is sensitive to temperature, density and interaction strength, but to first-order independent of the Wannier orbitals.

By comparing the results for soft-core and hard-core bosons in Fig. 2, one sees that the TG regime is approached for optical potentials $V_0/E_R = 9.5$ and $V_0/E_R = 12$, while it is fully reached only at $V_0/E_R = 20$, which in our model corresponds to a ratio $U/J = 259$. These values are in good agreement with Fig. 1, where the energy for $U/J = 200$ is only 4% lower than the energy of an ideal Fermi gas. For lower optical potentials, finite boson-boson interactions certainly need to be taken into account and double occupancies in the center of the trap do play an important role. We see in Fig. 2(e) that a Mott-like region is formed in the center of the trap. For a homogeneous system in the Mott phase, the dispersion relation of the excitations has a gap of order U [11], meaning that the role of double occupancies is strongly suppressed [13]. The Mott phase is entered at a ratio U/J as low as 1.67 at $T = 0$ for a density of one particle per site
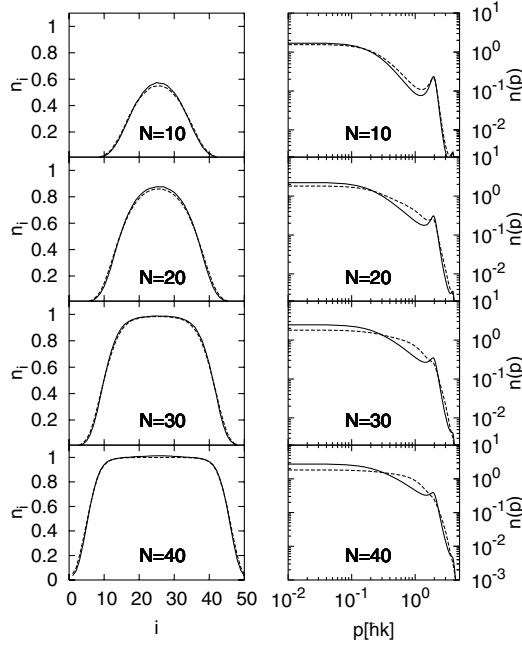
FIG. 3. Density profiles n_i and momentum density profiles $n(p)$ (p in units $\hbar k$) for different fillings N at an optical lattice potential $V_0/E_R = 7$ and temperature $T/J = 1$, for soft-core (solid line) and hard-core bosons (dashed line).

[25]. For the inhomogeneous system, the insulating behavior translates into a local compressibility that tends to vanish in the center of the trap [26]. Hence, for $T \ll U$ hard-core bosonic behavior can be reached for local densities varying from $\langle n_i \rangle = 0$ to $\langle n_i \rangle = 1$. However, the reduced local compressibility does not mean that for higher densities the TG regime would be reached at weaker optical-potential strengths. Figure 3 shows that a significant difference between the soft-core and hard-core momentum profiles persists even if the density profile develops a Mott-like region, at an intermediate optical lattice strength $V_0/E_R = 7$, ($U/J = 14.3$). This indicates that the short-range correlations in the Mott-like region differ significantly from the short-range correlations in the TG regime.

In conclusion, we have shown that the experiment of Ref. [6] is very well described by a Bose-Hubbard model based on Wannier orbitals. Soft-core boson wave functions with a significant contribution of double occupancies can explain the experimental results over the largest part of the optical-potential parameter range. Only for very deep optical lattices ($V_0/E_R = 20$) do the atoms behave as hard-core bosons and does the Tonks-Girardeau picture apply. The averaging over the array of one-dimensional tubes has only a minor effect and does not significantly alter the momentum profiles. At higher densities, Mott-like correlations might develop, but they do not enhance the convergence to the Tonks-Girardeau regime.

*Electronic address: Lode.Pollet@UGent.be
[1] D. Jaksch, C. Bruder, J. I. Cirac, C. W. Gardiner, and P. Zoller, Phys. Rev. Lett. **81**, 3108 (1998).
[2] M. Greiner, O. Mandel, T. Esslinger, T. W. Hänsch, and I. Bloch, Nature (London) **415**, 39 (2002).
[3] T. Stöferle, H. Moritz, C. Schori, M. Köhl, and T. Esslinger, Phys. Rev. Lett. **92**, 130403 (2004).
[4] M. Girardeau, J. Math. Phys. (N.Y.) **1**, 516 (1960).
[5] E. H. Lieb and W. Liniger, Phys. Rev. **130**, 1605 (1963).
[6] B. Paredes, A. Widera, V. Murg, O. Mandel, S. Fölling, I. Cirac, G. V. Shlyapnikov, T. W. Hänsch, and I. Bloch, Nature (London) **429**, 277 (2004).
[7] B. Laburthe Tolra, K. M. O'Hara, J. H. Huckans, W. D. Phillips, S. L. Rolston, and J. V. Porto, Phys. Rev. Lett. **92**, 190401 (2004).
[8] G. E. Astrakharchik, D. Blume, S. Giorgini, and B. E. Granger, J. Phys. B **37**, S205 (2004); G. E. Astrakharchik, J. Boronat, J. Casulleras, and S. Giorgini, cond-mat/0405225.
[9] M. Olshanii, Phys. Rev. Lett. **81**, 938 (1998).
[10] D. van Oosten, P. van der Straten, and H. T. C. Stoof, Phys. Rev. A **63**, 053601 (2001).
[11] M. P. A. Fisher, P. B. Weichman, G. Grinstein, and D. S. Fisher, Phys. Rev. B **40**, 546 (1989).
[12] D. B. M. Dickerscheid, D. van Oosten, P. J. H. Denteneer, and H. T. C. Stoof, Phys. Rev. A **68**, 043623 (2003).
[13] L. Pollet, S. Rombouts, K. Heyde, and J. Dukelsky, Phys. Rev. A **69**, 043601 (2004).
[14] C. Kollath, U. Schollwöck, J. von Delft, and W. Zwerger, Phys. Rev. A **69**, 031601(R) (2004).
[15] S. R. Clark and D. Jaksch, Phys. Rev. A **70**, 043612 (2004).
[16] S. Wessel, F. Alet, M. Troyer, and G. G. Batrouni, Phys. Rev. A (to be published).
[17] A. W. Sandvik, Phys. Rev. B **59**, R14157 (1999).
[18] L. Pollet, S. M. A. Rombouts, K. Van Houcke, and K. Heyde, Phys. Rev. E (to be published).
[19] O. F. Syljuåsen and A. W. Sandvik, Phys. Rev. E **66**, 046701 (2002); O. F. Syljuåsen, *ibid.* **67**, 046701 (2003).
[20] A. Dorneich and M. Troyer, Phys. Rev. E **64**, 066701 (2001).
[21] S. Sachdev, *Quantum Phase Transitions* (Cambridge University Press, Cambridge, England, 1999).
[22] M. A. Cazalilla, Phys. Rev. A **67**, 053606 (2003).
[23] Ch. Buggle, J. Léonard, W. von Klitzing, and J. T. M. Walraven, Phys. Rev. Lett. **93**, 173202 (2004).
[24] M. Olshanii and V. Dunjko, Phys. Rev. Lett. **91**, 090401 (2003); G. E. Astrakharchik and S. Giorgini, Phys. Rev. A **68**, 031602(R) (2003).
[25] T. D. Kühner, S. R. White, and H. Monien, Phys. Rev. B **61**, 12474 (2000).
[26] G. G. Batrouni, V. Rousseau, R. T. Scalettar, M. Rigol, A. Muramatsu, P. J. H. Denteneer, and M. Troyer, Phys. Rev. Lett. **89**, 117203 (2002).